PROCEEDINGS B

royalsocietypublishing.org/journal/rspb

Research

Cite this article: Mourlam MJ, Orliac MJ. 2019 Early evolution of the ossicular chain in Cetacea: into the middle ear gears of a semi-aquatic protocetid whale. *Proc. R. Soc. B* **286**: 20191417.
http://dx.doi.org/10.1098/rspb.2019.1417

Received: 17 June 2019
Accepted: 9 September 2019

Subject Category:
Palaeobiology

Subject Areas:
evolution, palaeontology

Keywords:
malleus, incus, stapes, archaeocetes, micro-computed tomography scan

Author for correspondence:
Mickaël J. Mourlam
e-mail: mickael.mourlam@umontpellier.fr

Electronic supplementary material is available online at https://doi.org/10.6084/m9.figshare.c.4668704.

THE ROYAL SOCIETY PUBLISHING

Early evolution of the ossicular chain in Cetacea: into the middle ear gears of a semi-aquatic protocetid whale

Mickaël J. Mourlam and Maeva J. Orliac

Institut des Sciences de l'Évolution, UMR 5554 CNRS, IRD, EPHE, Université de Montpellier, Place Eugène Bataillon, 34095 Montpellier cedex 5, France

MJM, 0000-0001-5631-2781; MJO, 0000-0002-8922-8356

Modifications of the morphology and acoustic properties of the ossicular chain are among the major changes that accompanied the adaptation of Cetacea to the aquatic environment. Thus, data on the middle ear ossicles of early whales are crucial clues to understand the first steps of the emblematic terrestrial/aquatic transition that occurred in that group. Yet, the delicate nature and very small size of these bones make their preservation in the fossil record extremely rare. Due to the scarcity of available data, major questions remain concerning the sound transmission pathways in early non-fully aquatic whales. Virtual reconstruction of a partially complete ossicular chain of an Eocene protocetid whale documents for the first time the three ossicles of a semi-aquatic archaeocete. Contrary to previous hypotheses, these ossicles present different evolutionary patterns, showing that the ossicular chain does not act as a single morphological module. Functional analyses of the different middle ear units highlight a mosaic pattern of terrestrial and aquatic signatures. This integrative anatomical and functional study brings strong evidence that protocetids were adapted to their dual acoustic environment with efficient hearing in both air and water.

1. Introduction

The adaptation to the aquatic environment by cetaceans implied drastic modifications of their sensory organs from their terrestrial ancestral condition. Among these, the sense of hearing was particularly reshaped in conjunction with the physical constraints imposed by water, implying modifications of the whole sound transmission pathway. The modality of the adaptation of the earliest cetaceans to underwater hearing is only partly known and major questions remain concerning hearing mechanisms in non-fully aquatic whales.

The delicate nature and very small size of the middle ear ossicles make their preservation in the fossil record rather unlikely; when preserved, all three ossicles are rarely found together and almost never in their anatomical position. Yet, few middle ear ossicles are documented for non-fully aquatic early whales. The incus of the earliest archaeocete *Pakicetus* (early Eocene, Pakistan) [1] documents the oldest cetacean ossicle and shows an intermediate morphology between terrestrial artiodactyls and cetaceans (e.g. incomplete rotation of the ossicular chain [1]). In addition, the ossicular chain is nearly fully known for remingtonocetids (one *in situ* ossicular chain and one incudomallear complex of *Remingtonocetus*; middle Eocene, India [2,3]) and only partially documented for protocetids (two partially preserved mallei; middle Eocene, India [2,3]). Based on this incomplete record, some authors concluded that underwater hearing in these early whales was almost fully functional, while aerial hearing was strongly altered [2,4]. Middle ear ossicles of extinct, strictly aquatic early whales, such as basilosaurids, are well documented [5–8]. They display the derived morphology observed in modern cetaceans [5,6,9,10], strongly suggesting fully functional underwater hearing abilities.

Micro-computed tomography (CT) scan investigation of the middle ear cavity of a protocetid whale partial cranium (Lutetian, Togo [11,12]) provides unprecedented access to the partially complete ossicular chain (composed of malleus, incus and stapes) of this amphibious archaeocete whale. This discovery provides essential clues for understanding the functioning of the ear of a semi-aquatic cetacean and to discuss the early evolutionary history of the sound transmission pathway in Cetacea.

(a) Institutional abbreviations

H-GSP, Howard University, Geological Survey of Pakistan; LSUMG, Louisiana State University, Museum of Geoscience, Baton Rouge, Louisiana, USA; MRAC, Musée Royal d'Afrique Centrale, Tervuren, Belgium; NOAA, National Oceanic and Atmospheric Administration, Southwest Fisheries Science Center, Washington, DC, USA; UBC, University of British Columbia, Vancouver, Canada; UM, Université de Montpellier, France.

2. Material and methods

(a) Material

The specimen UM-KPG-M 73, investigated in this study, was collected in Lutetian phosphate deposits (*ca* 46–43 Ma) at Kpogamé, Togo [11,12]. It consists of a skull fragment of an adult protocetid belonging to an indeterminate species, referred to as 'morphotype *γ*' by Mourlam & Orliac [12]. Micro-CT scan investigation revealed the presence of the almost complete ossicular chain: the stapes and the incus are finely preserved, whereas the malleus was damaged during the physical preparation of the specimen [11]. In order to facilitate anatomical comparisons, we provide a simplified 'incudomalleo-centred' orientation system considering the two articular facets as referential (see electronic supplementary material, text S1 and figure S1). Detailed descriptions of the petrotympanic complex and bony labyrinth of Protocetidae indet *γ* were provided by Mourlam & Orliac [12,13].

(b) Micro-computed tomography scan investigation

UM-KPG-M 73 was scanned with a resolution of 70 µm using a General Electric Phoenix Nanotom S at the AniRA-ImmOs (SFR Biosciences Gerland-Lyon) microtomography facility. The three ossicles were virtually extracted manually slice by slice using the segmentation tools of AVIZO 9.0 [14]. No smoothing was performed in the rendering process for the surfaces used in the following analyses (see [15]). Three-dimensional models are available at MorphoMuseuM.com (tympanic bulla, M3#134_UM KPG-M 73; stapes, M3#407_UM KPG-M 73; incus, M3#408_UM KPG-M 73; malleus, M3#409_UM KPG-M 73).

(c) Hearing parameters measurement

Linear measurements follow Uhen ([8], fig. 48) and Hemilä *et al.* ([16], pp. 33–34) for the lever arm lengths. The volume of the incus and stapes were measured with AVIZO 9.0 [14] and their estimated mass ranges follow Nummela *et al.* [2,3] considering a minimum ossicular bone density of 2.0 g cm^{-3}, based on terrestrial mammals, and a maximum of 2.7 g cm^{-3}, based on odontocetes. Bone thickness quantification of the tympanic bulla was computed as the minimum Euclidean distance between a mesh node of the outer tympanic surface and a mesh triangle of the inner tympanic surface [17–19] using the 'Surface Distance' tools of AVIZO 9.0 [14]. The resultant matrix was used to generate a 3D chromatic map with its associated isopleth bone thickness information [20]. The tympanic plate area has been estimated following Nummela *et al.* [21] and the isopleth of 2 mm. Above this value, thickness of the tympanic bone increases markedly (see electronic supplementary material, figure S2). The estimation of the tympanic membrane area follows Nummela [22] and includes the pars flaccida (electronic supplementary material, figure S3). All surface areas were taken using the measurement tools of Fiji [23]. Measurement of sound input areas (*sensu* [2,3]) along with the incudal and stapedial masses of other mammals (see electronic supplementary material, table S1) have been compiled from Nummela [22] and Nummela *et al.* [2,3,21], to which we added data for *Choeropsis liberiensis* (MRAC RG 35715) and *Delphinus capensis* (NOAA-cet 436B-KXD0307). Mallear and incudal lever arm lengths data come from Hemilä *et al.* [16] and the geometric transformer ratio of the middle ear has been computed following these authors (i.e. product between the area ratio ((tympanic membrane area × 2/3)/fenestra vestibuli area) and the lever arm ratio (length of mallear lever arm/length of incudal lever arm)).

3. Results

(a) Description and comparisons

The partially complete ossicular chain of UM-KPG-M 73 is preserved in the middle ear cavity (figure 1*a*). The stapes is close to its original anatomical position and the natural articulation between the incus and malleus appears to be roughly maintained. However, the incudomallear complex moved post-mortem and it is not possible to provide a robust reconstruction of the original position of the ossicular chain due to the partial preservation of the auditory region (electronic supplementary material, text S1).

(i) Stapes

The stapes, partially sunk (post-mortem) within the bony labyrinth, has kept its original anteroposterior orientation (figure 1*b–e*). Compared with available data on early whales, the UM-KPG-M 73 stapes is lightly built, with very thin crura of the same width, and it does not show the pachyostosis observed in basilosaurids and extant cetaceans [5,6,8] (electronic supplementary material, figure S4). It is high and narrow, and bears a wide foramen intercrurale of the same diameter on both faces. The capitulum is broad and presents a large articular facet for the contact with the crus longum of the incus [24–26]. Its long axis does not have the same orientation as that of the stapedial footplate (figure 1*e*). The distinction between the capitulum and the crura is clearly marked by a neck, contrary to the artiodactyl sample described by Orliac & Billet ([15], fig. 2) and to the fully aquatic cetaceans [6,8,26,27]. The muscular process, serving as attachment site for the stapedial muscle and located on the posterior crus, is wide and blunt. The footplate, articulating with the petrosal at the fenestra vestibuli, is oblong with a stapedial ratio of 1.42. It is fully concave on the vestibular face, like basilosaurids and modern cetaceans [24,28], and unlike non-cetacean artiodactyls. The concave vestibular face of the stapedial footplate is concurrent with an increase in the footplate thickness near the base of the two crura.

(ii) Incus

In ventral view, the incus is stocky and conical in shape, slightly compressed anteroposteriorly (figure 1*f–i*). The

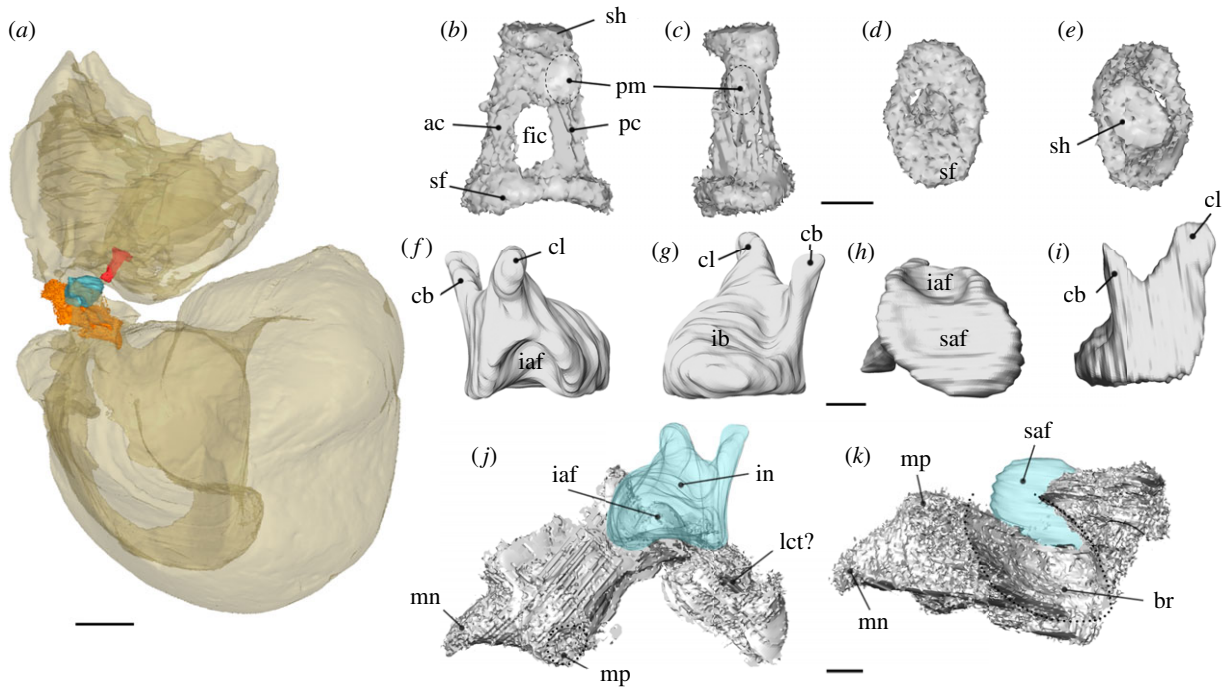

Figure 1. Three-dimensional models of the partially complete left ossicular chain of protocetid indeterminate γ (UM-KPG-M 73). (*a*) Location of the ossicular chain preserved within the middle ear cavity in the anterior view (red, stapes; blue, incus; orange, malleus; bony transparent elements, petrosal on top and tympanic bulla underneath). (*b–e*) Stapes in, from left to right, medial, posterior, dorsal and ventral views. (*f–i*) Incus in, from left to right, ventral, dorsal, anterior and lateral views. (*j–k*) Malleus in (*j*) dorsal and (*k*) anterior views. The orientation of incus and malleus based on a spatial 'incudomallear-centred' referential (see electronic supplementary material, text S1 and figure S1). ac, anterior crus; br, broken or incomplete structure; cb, crus breve; cl, crus longum; fic, foramen intercrurale; iaf, inferior articular facet; ib, incudal body; in, incus; lct, lodge of the lateral extension of the chorda tympani; mn, manubrium; mp, muscular process of malleus; pc, posterior crus; pm, processus muscularis stapedis; saf, superior articular facet; sf, stapedial footplate; sh, head of stapes. Scale bar in (*a*), 1 cm; other scale bars, 1 mm. (Online version in colour.)

incus of UM-KPG-M 73 is of 'cetacean type' and presents several characters retrieved in cetaceans (electronic supplementary material, figure S5): (i) the size and orientation of the crura are of cetacean type with a posteriorly oriented larger crus longum extending from the inferior articular facet and a more lateral, thinner, crus breve [26,29]; (ii) the strong size difference between the facets of the articular surface for the malleus is typical of what is observed in cetaceans [1,6,25]; and (iii) the angulation of the two articular facets is positioned at a right angle [5,8,27,30]. Among Cetacea, the incus of UM-KPG-M 73 is morphologically closer to that of *Pakicetus* than that of remingtonocetids and pelagicetes (basilosaurids and neocetes *sensu* [31]), with: (i) no inflation of the incudal body; (ii) slight inflation of the crus longum; and (iii) a posterior location of the base of the crus breve.

(iii) Malleus

The malleus was damaged during the preparation of the specimen (mechanical abrasion of body and head; figure 1*j–k*). Nevertheless, the convex inferior articular facet and part of the superior articular facet are intact. The former facet matches its counterpart on the incus (figure 1*j*), which allows assessment of the whole shape of the articular surface (electronic supplementary material, figure S6). The malleus was broad and pachyostotic. The lateral part of the mallear head is perforated by a wide canal that we interpret as part of the lodge of the lateral extension of the chorda tympani (electronic supplementary material, text S2 and figure S7). On the mallear body, the gonial was completely abraded by mechanical preparation. In dorsal view, medial to the main broken area, a tuberosity surmounted by a small circular pit (dotted line in figure 1*j*) corresponds to the muscular process, which is the site of insertion for the tendon of the tensor tympani muscle [6,26,32]. The mallear body bears a short hook-like manubrium.

The malleus of UM-KPG-M 73 is closer to Pelagiceti than to its terrestrial relatives (electronic supplementary material, figures S6 and S8): the muscular process is small and blunt instead of spike-like, the manubrium is short, and the chorda tympani probably passes through the mallear head. Based on the preserved structures, the general shape and dimensions of UM-KPG-M 73 malleus are also close to the protocetid *Indocetus ramani* and the remingtonocetid *Remingtonocetus* sp. ([3], fig. 2E–G).

(b) Ecoacoustic niche investigation

Various isometric correlations have been found between the different components of the sound transmission chain, from the outer/middle ear interface (*sensu* [2,3]) to the middle/inner ear interface [21,22]. Since the middle ear is acting as an impedance matching device, these correlations are dependent on the soundtope (i.e. living environment of uniform acoustic conditions; see also [33]) of a taxon and are therefore informative ecological proxies [2,3]. Figure 2 presents a mechanical dissection of the middle ear of UM-KPG-M 73 through a set of correlations between different links in the sound transmission chain, from the sound input area (sound wave entrance to the middle ear; see [2,3]) to the fenestra vestibuli (sound wave entrance to the inner ear). Figure 2*a*,*b* represents the distribution of incudal mass (figure 2*a*) values and fenestra vestibuli area (figure 2*b*), respectively, relative to sound

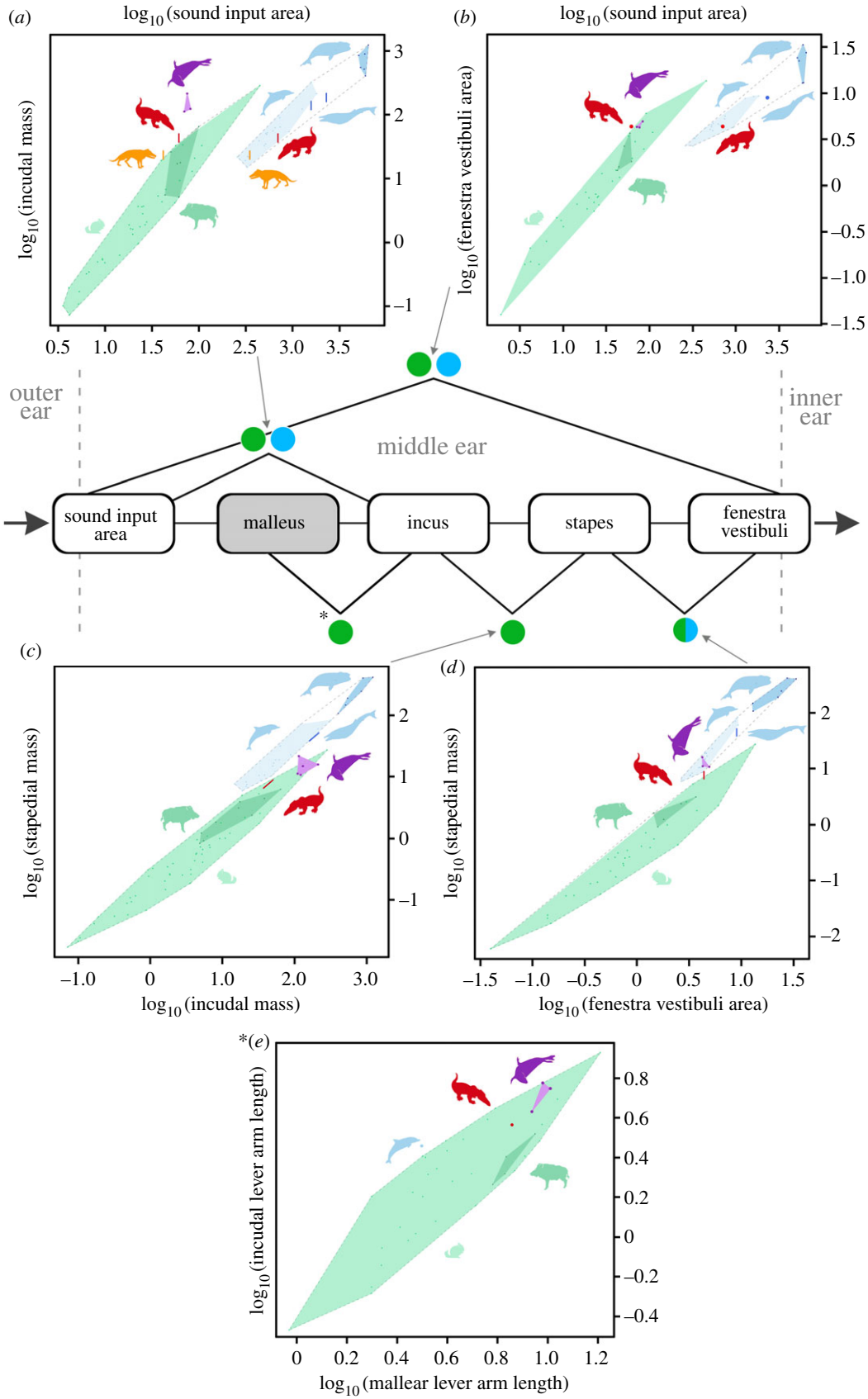

Figure 2. Mechanical dissection of the middle ear of protocetid indeterminate γ (UM-KPG-M 73). Set of bivariate plots: (*a*) incudal mass versus sound input area; (*b*) fenestra vestibuli area versus sound input area; (*c*) stapedial mass versus incudal mass; (*d*) stapedial mass versus fenestra vestibuli area; (*e*) incudal lever arm length versus mallear lever arm length. Measurements are available in electronic supplementary material, table S1. The grey dotted lines outline the morphospace of terrestrial mammals and that of neocetes. Blue silhouettes, pelagicetes; dark blue dots, mysticetes; light blue dots, odontocetes; navy blue dots or lines, basilosaurids (including at least *Basilosaurus cetoides* (LSUMG V1)); dark green, non-cetaceans artiodactyls; light green, terrestrial mammals excluding artiodactyls; orange, *Pakicetus* (H-GSP 91035); purple, phocids; red, protocetid indeterminate γ (UM-KPG-M 73). Illustrations by R. Mourlam. The results of these five analyses are summed up in the functional profile of the middle ear of protocetid indeterminate γ (UM-KPG-M 73) at the centre of this figure. Each pair of links is symbolized by a circle. The asterisk next to the circle between the malleus and the incus refers to the corresponding graph (*e*). The double circles stand for the double sound input area (tympanic membrane and tympanic plate). In green, functional aerial hearing; in cyan, functional underwater hearing. Damaged malleus is symbolized in grey (see also electronic supplementary material, figure S9). (Online version in colour.)

input area for fully terrestrial mammals and phocids (sound input area = tympanic membrane surface) and for cetaceans (sound input area = tympanic plate surface, following [2,3,21]). According to both plots, based on its tympanic membrane surface, UM-KPG-M 73 lies slightly above the terrestrial mammals' morphospace, whereas it lies within the odontocetes' morphospace according to its tympanic plate area, suggesting optimal hearing abilities both in air and underwater. Interestingly, based on the measurements provided by Nummela *et al*. [3], *Pakicetus* follows the same pattern (figure 2*a*) and lies on the edge of the terrestrial's morphospace (tympanic membrane area), close to UM-KPG-M 73, and within the odontocetes' morphospace (tympanic plate area). This suggests that *Pakicetus* also had middle ear proportions suited to hear in air and underwater. As already shown in previous studies [2,3], based on their tympanic plate surface, the basilosaurids *Zygorhiza* and *Basilosaurus* are found within the cetaceans' morphospace, between odontocetes and mysticetes. Yet, no data are available for the tympanic membrane surface of basilosaurid and their aerial hearing abilities could not be investigated here.

Within the ossicular chain and at the end of the sound transmission pathway (figure 2*c–e*), UM-KPG-M 73 shows a rather terrestrial signature. According to the relative mass of the incus and stapes (figure 2*c*), it lies within the terrestrial's morphospace, halfway between artiodactyls and cetaceans. When the mass of the stapes relative to the fenestra vestibuli area is considered, UM-KPG-M 73 is found between the terrestrial and modern cetaceans' morphospaces (figure 2*d*). In addition, according to the relative proportion of the length of the two lever arms of the incudomallear complex [16], the protocetid lies within the terrestrial morphospace, where it is located halfway between artiodactyls and phocids (figure 2*e*). Modern cetaceans possess a different lever mechanism [34–36] and there are, to our knowledge, no available data in the literature to directly compare this parameter with that of terrestrial mammals. Nevertheless, according to our measurements of the two lever arms on the incudomallear complex of *D. capensis*, this odontocete is found out of the terrestrial mammals' morphospace (figure 2*e*). Finally, for comparison purposes, the geometric transformer ratio (*sensu* [16]; see 'Material and methods' and also [37,38]) of UM-KPG-M 73 is 18.7, which is lower than most terrestrial mammals (see electronic supplementary material, table S1) and close to that of phocids (transformer ratio between 19.20 and 22.35) and human (transformer ratio = 21.38).

4. Discussion

(a) Early evolutionary history of the ossicular chain in Cetacea

The preservation of a partially complete protocetid ossicular chain represents a unique opportunity to document the sound transmission pathway in a non-fully aquatic cetacean and to refine the current knowledge on their early evolutionary history. The stapes is morphologically close to terrestrial artiodactyls and does not show the pachyostosis observed in fully aquatic cetaceans (basilosaurids and neocetes). Likewise, the incus body is only slightly inflated and shows proportions similar to *Pakicetus* or modern hippos. On the other hand, the preserved portions of the malleus indicate that it was composed of a massive pachyostotic head, morphologically close to the basilosaurid condition. Hence, the stapes and the incus do not show the same bulkiness as the malleus, which goes against the hypothesis postulated by Fleischer [25] and Lancaster [6] that the three ossicles acquired cetacean characters (among which pachyostosis) all together, as a single evolutionary unit. The decoupling of acquisition of derived functional characters between the different links of the ossicular chain is illustrated in figure 3, which shows, in a phylogenetic context, the repartition of morphological characters for the three ossicles, at the Cetancodonta [39–41] scale. The ossicular chain of UM-KPG-M 73 indeed shows a mosaic of plesiomorphic and derived characters, with a pachyostotic malleus (first link of the chain) and no to little pachyostosis of the incus and stapes (second and last link of the chain). The fully pachyostotic condition of the three ossicles is observed in basilosaurids [5,6,8] and neocetes [24,42–52] at the Pelagiceti node, and could be related to strictly underwater hearing in cetes.

The early evolutionary history of the cetacean's auditory region is also marked by the rotation of the ossicular chain [1,6,25,53]. Despite damage on the tympanic bulla, petrosal and malleus of UM-KPG-M 73 (see 'Description and comparisons' and electronic supplementary material, text S1), some anatomical elements of the incus provide evidence that the rotation of the incudomallear complex was similar to that of *Pakicetus* [1] and intermediate between fully terrestrial artiodactyls and cetaceans. Indeed, compared to terrestrial artiodactyls, the two crura of the incus of UM-KPG-M 73 show a rotated position relative to the articular surface (figure 3, character I3, turquoise state) and a change of their relative proportions (figure 3, character I2, turquoise state). The rotation of the incudomallear complex is also accompanied by drastic changes of body proportions of the malleus (figure 3, character M1) and of the shape of its manubrium (figure 3, character M2). The malleus of UM-KPG-M 73 is intermediate in terms of body proportions and similar to some modern cetaceans in terms of manubrium size (e.g. *Balaenoptera musculus* ([54], pl. 74) and *Eubalaena australis* ([28], pl. 63). In addition to these characters (which states vary within Cetacea), three others are common to all cetaceans of our sample: a large difference in size between the superior and inferior articular facets of the malleus (figure 3, character M3, blue state), a right angle between these two facets and a concave stapedial footplate (figure 3, character S2, blue state). It is noteworthy that among Artiodactyla, *C. liberiensis* (figure 3; electronic supplementary material, figures S5G and S8C) and probably *Hippopotamus amphibius* ([28], pl. 61) present the same 'cetacean' structural organization of their incudomallear articular surface, indicating either an amphibious hearing signal (functional convergence) or a potential osteological synapomorphy for Cetancodonta [39,41,55].

Contrary to previous hypotheses, we show here that the ossicular chain of UM-KPG-M 73 does not act as a single morphological module [56–58] within the middle ear. The mosaic pattern of character states (figure 3) shows a relative independence of evolutionary tempo and mode (*sensu* [59]) between the different ossicles, with a rather plesiomorphic stapes and a more derived malleus. This morphological modularity can be explained by the fact that the stapes derives from the hyoid arch (second pharyngeal arch), whereas the

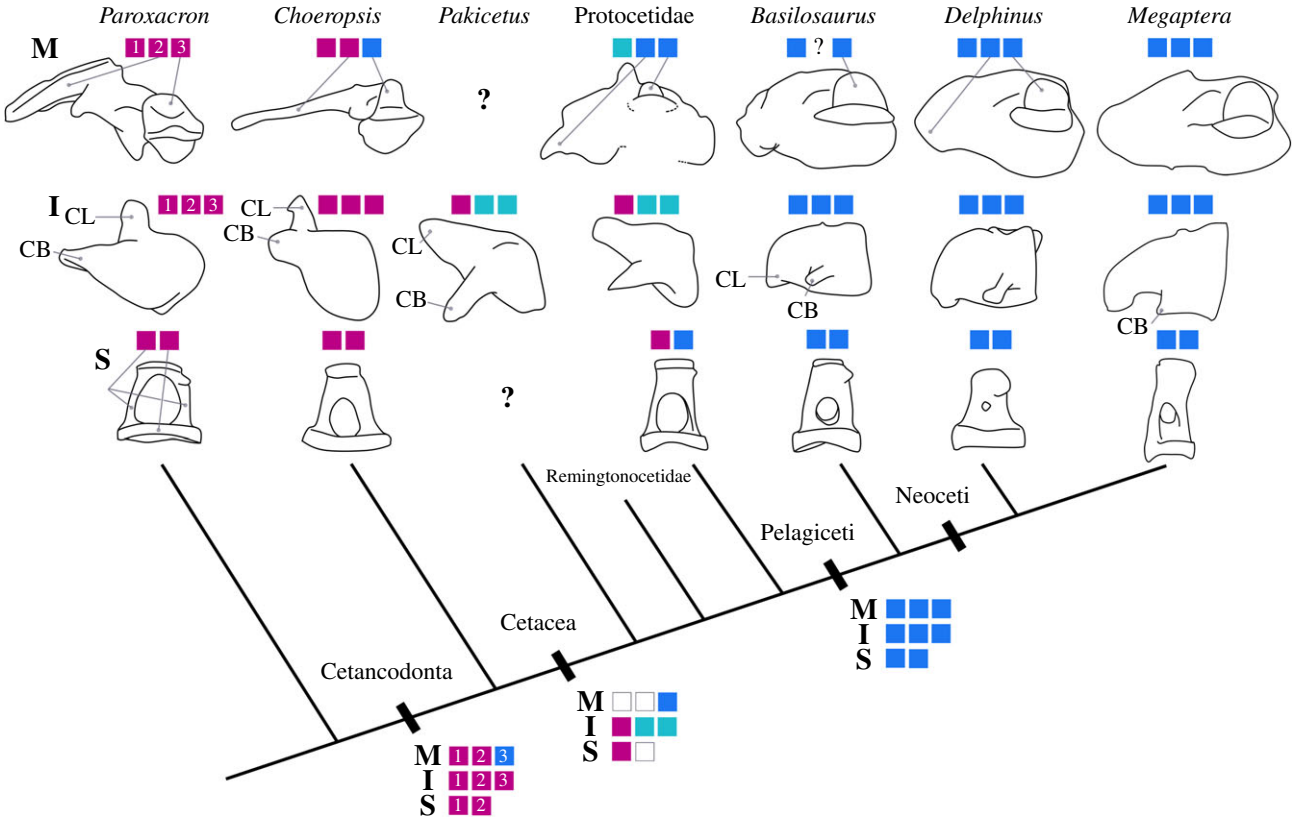

Figure 3. Evolution of some characters of the ossicular chain components, malleus (M), incus (I) and stapes (S), character states of terrestrial artiodactyls are in pink, character states found in fully aquatic cetaceans are in blue and intermediate states are in turquoise. Character list: S1, crura pachyostosis (pink, absent; blue present); S2, stapedial footplate (pink, convex or flat; blue, concave); I1, inflation of the body (pink, no inflation; turquoise, moderate; blue, important); I2, relative size of crus longum versus crus breve (pink, crus breve bigger; turquoise, crus breve smaller; blue, crus breve much smaller); I3, reorientation of crura relative to the articular surface (pink, no rotation; turquoise, intermediate rotation of the crura; blue, full rotation of the crura); M1, proportions (pink, body longer; turquoise, body and head of relative similar length; blue, head longer); M2, manubrium shape (pink, long process; blue, from a hook-like process to a vestigial site of insertion for the tympanic ligament); M3, relative size of articular facets (pink, subequal; blue, inferior articular facet smaller than the superior). CB, crus breve; CL, crus longum. Question marks represent missing data and white boxes represent character state ambiguity related to missing data for *Pakicetus*. Ossicles not to scale. *Megaptera novaeangliae* malleus, stapes (UBC-cet 416B 16-4358) and incus after Bosselaers & Post ([49], fig. 12). Information related to other specimens illustrated is provided in the 'Material and methods' section and in the anatomical plates of the electronic supplementary material. (Online version in colour.)

incudomallear complex originates from the mandibular arch (first pharyngeal arch) [60,61]. In addition, the incus and malleus derive from two different bone units, the quadrate and articular, respectively [25,62–65]. Moreover, even within a single ossicle, a combination of derived and plesiomorphic character states is always observed (i.e. different modules can be identified within the same ossicle; figure 3). At that level of integration (i.e. intra-bone), data on the development of the mammalian middle ear are rather limited and mainly rely on mice [66]. However, two modules have been identified within the stapes of these rodents: the outer edge of the footplate derives from the otic capsule (mesoderm origin), whereas the rest of this ossicle comes from the neural crest [66,67]. These different developmental origins could explain the mosaic pattern of characters of the protocetid stapes.

(b) Functional profile of the protocetid amphibious middle ear

Every medium has its own resistance to sound transmission. This resistance is called the acoustic impedance (Z), and can be quantified as the ratio between sound pressure (p) and particle velocity (v) (i.e. $Z = p/v$) [3,16,68]. At the interface between two different media, the less their acoustic impedance differs, the better the sound is transmitted. The hearing mechanism consists in sound transmission between the external environment, where sound waves are born, and the internal environment of the inner ear, where sound waves are transduced into electrical signals transmitted to the brain. The acoustic impedance of the fluid-filled cochlea of the inner ear is about 10 times lower than that of water and 375 times higher than that of air [4,36,69]. These large differences of acoustic impedance between the soundtope and the inner ear prevent a direct transmission of sound (most of the acoustic energy would be lost at their interface through sound reflection; see [36,69]). In tetrapods, the middle ear plays an essential role in hearing by minimizing the acoustic impedance mismatch between the soundtope and the inner ear [16,38,70,71]. The sound pressure depends mainly on the ratio between the sound input area (tympanic membrane or tympanic plate) and the surface of the fenestra vestibuli, while the particle velocity relies on different lever arms [16,36,38,70]. Thus, to match a low acoustic impedance soundtope (air) with the fluid-filled cochlea, the role of the middle ear will be to increase sound pressure and decrease particle velocity. The contrary goes for matching a high acoustic impedance soundtope (water) with the inner ear [4,68]. Consequently, at first glance, it seems counterintuitive

that a single sound transmission pathway could be tuned for both airborne and waterborne sounds (i.e. being able to increase and decrease simultaneously sound pressure).

The assessment, for the first time, of a partially complete middle ear of a non-fully aquatic archaeocete enhances our understanding of amphibious hearing in early whales. The anatomical survey of the tympanic bulla of UM-KPG-M 73 highlights the presence of two potential sound input areas [12]: (i) the tympanic membrane, collecting sound from air; (ii) the tympanic plate, for underwater sound. This duality of potential sound input area provides two independent possibilities to regulate sound pressure through the sound transmission pathway within the middle ear. In air, the ear of UM-KPG-M 73 functioned the same way as terrestrial mammals. The tympanic membrane area is broader than that of the fenestra vestibuli, which implies an increase in sound pressure within the sound transmission chain. In parallel, the lever ratio between the mallear and incudal lever arms of UM-KPG-M 73 is typical of that of land mammals (figure 2*e*) [16], indicating a decrease in particle velocity. By contrast, the geometric transformer ratio (*sensu* [16]) of UM-KPG-M 73 is lower than that of most land mammals and similar to that of phocids (see electronic supplementary material, table S1), probably in relation with their amphibious lifestyle. Underwater, the ear of UM-KPG-M 73 functioned in a way close to modern cetaceans. The surface of the tympanic plate is broader than that of the fenestra vestibuli, which increases sound pressure within the middle ear. However, as explained above, sound pressure should be decreased to avoid impedance mismatch between water and the cochlea. Thus, to compensate the sound pressure increase induced by the tympanic plate surface, particle velocity should be even more increased. Hemilä *et al*. [36] propose two lever mechanisms involving the tympanic bulla and the ossicular chain that would be able to increase particle velocity within modern cetacean's middle ear. Unfortunately, in UM-KPG-M 73, the gonial and part of the tympanic plate are broken, and it is not possible to quantify these parameters. Nevertheless, based on strong morphological similarities and equivalent sound pressure ratio (figure 2*b*), the middle ear of UM-KPG-M 73 probably performed an efficient acoustic impedance matching between the aquatic soundtope and the inner ear, such as that of modern odontocetes.

This mosaic functional profile of the middle ear is also observed in phocids (figure 2; electronic supplementary material, figure S9) that are able to hear efficiently in both aquatic and aerial soundtopes [72–78]. Although phocids and UM-KPG-M 73 present different morphological adaptations towards amphibious hearing (such as a strong increase in incudal mass for the former [69] and a potential double sound input area for the latter), their middle ears' functional profiles are very similar. The patchwork of functional signals observed in these two phylogenetically distant groups appears to be a hallmark of the mammalian amphibious ear.

5. Summary and conclusions

The anatomical and functional studies of the first partially complete protocetid middle ear support the amphibious hearing signal found with the cochlea of its inner ear [13]. Functional analyses of the different links of the sound transmission pathway within the middle ear highlight a combination of aerial and aquatic signals (figure 2; electronic supplementary material, figure S9). This indicates that the ossicular chain is able to process the sound coming from the two acoustic portals of the bulla (tympanic membrane and tympanic plate) and to transmit sound waves efficiently to the inner ear. This functional duality is tightly linked with the morphology of the three ossicles that present a mosaic of plesiomorphic (terrestrial artiodactyl) and derived (fully aquatic cetacean) character states (figures 1 and 3). Indeed, the morphological modularity of the ossicular chain increases the adaptability of the protocetid's hearing organ [38,56–58,60], and thus makes it possible for a unique middle ear to be in tune with two soundtopes with drastically different physico-acoustic properties.

Data accessibility. Additional data relating to this study are available from the Dryad Digital Repository: https://dx.doi.org/10.5061/dryad.0k3fv2j [79]. Three-dimensional models of the three ossicles and the tympanic bulla of UM-KPG-M 73 are available at: https://morphomuseum.com/ (tympanic bulla, M3#134_UM KPG-M 73; stapes, M3#407_UM KPG-M 73; incus, M3#408_UM KPG-M 73; malleus, M3#409_UM KPG-M 73).

Authors' contributions. M.J.M. and M.J.O. conceived and designed the study. M.J.O. performed the data segmentation and M.J.M. performed the functional analyses. Both authors wrote the manuscript.

Competing interests. We declare we have no competing interests.

Funding. This study was supported by the ANR/ERC funding project PALASIAFRICA, headed by L. Marivaux; the ANR programme SPLASH (no. ANR-15-CE32-0010-01), headed by J.-R. Boisserie and F. Lihoreau; and the CeMEB project PygmHippoCom (coPi M. J. Orliac).

Acknowledgements. We are especially grateful to J. G. M. Thewissen (NEOMED) for access to 3D models of the ossicles of *Pakicetus* and *Basilosaurus*, to S. Usip and D. A. Waugh from NEOMED for the scans of these specimens, to K. Danil (NOAA-Southwest Fisheries Science Center) for collecting and preparing the middle ear of *Delphinus* and to M. Morell (Institute for Neurosciences of Montpellier, France—Inserm Unit 1051) for providing us with the scan of this specimen along with that of *Megaptera*. We also acknowledge S. Raverty (Animal Health Center, Canada), who helped M. Morell extracting the ear of *Megaptera*. We are grateful to M. Bouchet, C. Charles and J. Martin for access to the AniRA-ImmOs (SFR Biosciences Gerland-Lyon) microtomography facility. We acknowledge the MRI platform member of the national infrastructure France-BioImaging supported by the French National Research Agency (ANR-10-INBS-04, 'Investments for the future'), the labex CEMEB (ANR-10-LABX-0004) and NUMEV (ANR-10-LABX-0020). We are also very grateful to P.-O. Antoine for his comments and to R. Mourlam for her help in improving the English of the manuscript, along with her illustrations of archaeocetes and other mammals. We also thank the three anonymous reviewers, who greatly helped to improve this article. This is ISE-M publication no. ISEM 2019-137.

References

1. Thewissen JGM, Hussain ST. 1993 Origin of underwater hearing in whales. *Nature* **361**, 444–445. (doi:10.1038/361444a0)

2. Nummela S, Thewissen JGM, Bajpai S, Hussain ST, Kumar K. 2004 Eocene evolution of whale hearing. *Nature* **430**, 776–778. (doi:10.1038/nature02720)

3. Nummela S, Thewissen JGM, Bajpai S, Hussain ST, Kumar K. 2007 Sound transmission in archaic and modern whales: anatomical adaptations for

underwater hearing. *Anat. Rec.* **290**, 716–733. (doi:10.1002/ar.20528)

4. Nummela S, Yamato M. 2018 Hearing. In *Encyclopedia of marine mammals* (eds B Würsig, JGM Thewissen, KM Kovacs), pp. 462–470. Amsterdam, The Netherlands: Elsevier.
5. Pompeckj JF. 1922 Das Ohrskelett von Zeuglodon. *Senckenbergiana* **3**, 44–100.
6. Lancaster WC. 1990 The middle ear of the Archaeoceti. *J. Vertebr. Paleontol.* **10**, 117–127. (doi:10.1080/02724634.1990.10011795)
7. Gingerich PD, Uhen MD. 1996 *Ancalecetus simonsi*, a new Dorudontine Archaeocete (Mammalia, Cetacea) from the Early Late Eocene of Wadi Hitan, Egypt. *Contrib.Mus. Paleontol. Univ. Michigan* **29**, 359–401. (doi:10.1111/j.1748-7692.2001.tb00979.x)
8. Uhen MD. 2004 Form, function, and anatomy of *Dorudon atrox* (Mammalia, Cetacea): an archaeocete from the Middle to Late Eocene of Egypt. *Univ. Michigan Pap. Paleontol.* **34**, 1–222.
9. Kellogg R. 1936 A review of the Archaeoceti. *Carnegie Inst. Washingt.* **482**, 1–366.
10. Oelschläger HA. 1990 Evolutionary morphology and acoustics in the dolphin skull. In *Sensory abilities of cetaceans* (eds JA Thomas, RA Kastelein), pp. 137–162. Boston, MA: Springer US.
11. Gingerich PD, Cappetta H. 2014 A new archaeocete and other marine mammals (Cetacea and Sirenia) from lower middle Eocene phosphate deposits of Togo. *J. Paleontol.* **88**, 109–129. (doi:10.1666/13-040)
12. Mourlam MJ, Orliac MJ. 2018 Protocetid (Cetacea, Artiodactyla) bullae and petrosals from the middle Eocene locality of Kpogamé, Togo: new insights into the early history of cetacean hearing. *J. Syst. Palaeontol.* **16**, 621–644. (doi:10.1080/14772019.2017.1328378)
13. Mourlam MJ, Orliac MJ. 2017 Infrasonic and ultrasonic hearing evolved after the emergence of modern whales. *Curr. Biol.* **27**, 1776–1781. (doi:10.1016/j.cub.2017.04.061)
14. Visualization Sciences Group. 2018 Avizo: 3D analysis software for scientific and industrial data. See www.fei.com/software/avizo.
15. Orliac MJ, Billet G. 2016 Fallen in a dead ear: intralabyrinthine preservation of stapes in fossil artiodactyls. *Palaeovertebrata* **40**, 1–10. (doi:10.18563/pv.40.1.e3)
16. Hemilä S, Nummela S, Reuter T. 1995 What middle ear parameters tell about impedance matching and high frequency hearing. *Hear. Res.* **85**, 31–44. (doi:10.1016/0378-5955(95)00031-X)
17. Guy F, Gouvard F, Boistel R, Euriat A, Lazzari V. 2013 Prospective in (Primate) dental analysis through tooth 3D topographical quantification. *PLoS ONE* **8**, e66142. (doi:10.1371/journal.pone.0066142)
18. Lazzari V, Guy F. 2014 Quantitative three-dimensional topography in taxonomy applied to the dental morphology of catarrhines. *BMSAP* **26**, 140–146. (doi:10.1007/s13219-014-0099-9)
19. Thiery G, Lazzari V, Ramdarshan A, Guy F. 2017 Beyond the map: enamel distribution characterized from 3D dental topography. *Front. Physiol.* **8**, 1–12. (doi:10.3389/fphys.2017.00524)
20. Lazzari V, Tafforeau P, Aguilar J-P, Michaux J. 2008 Topographic maps applied to comparative molar morphology: the case of murine and cricetine dental plans (Rodentia, Muroidea). *Paleobiology* **34**, 46–64. (doi:10.1666/06052.1)
21. Nummela S, Wägar T, Hemilä S, Reuter T. 1999 Scaling of the cetacean middle ear. *Hear. Res.* **133**, 71–81. (doi:10.1016/S0378-5955(99)00054-4)
22. Nummela S. 1995 Scaling of the mammalian middle ear. *Hear. Res.* **85**, 18–30. (doi:10.1016/0378-5955(95)00030-8)
23. Schindelin J *et al.* 2012 Fiji: an open-source platform for biological-image analysis. *Nat. Methods* **9**, 676–682. (doi:10.1038/nmeth.2019)
24. Kellogg R. 1927 *Kentriodon pernix*, a Miocene porpoise from Maryland. *Proc. United States Nat. Mus.* **69**, 1–55. (doi:10.5479/si.00963801.69-2645.1)
25. Fleischer G. 1978 Evolutionary Principles of the Mammalian Middle Ear. *Adv. Anat., Embryol. Cell Biol.* **55**, 1–70. (doi:10.1007/978-3-642-67143-2)
26. Mead JG, Fordyce RE. 2009 The therian skull: a lexicon with emphasis on the odontocetes. *Smithson. Contrib. Zool.* **627**, 1–249. (doi:10.5479/si.00810282.627)
27. Fraser FC, Purves PE. 1960 Hearing in cetaceans. *Bull. Br. Mus. (Nat. Hist. Zool.)* **7**, 1–140.
28. Doran AHG. 1878 XVIII. Morphology of the mammalian *Ossicula auditûs*. *Trans. Linn. Soc. Lond. 2nd Ser. Zool.* **1**, 371–497. (doi:10.1111/j.1096-3642.1878.tb00663.x)
29. Lambert O, Bianucci G, de Muizon C. 2016 Macroraptorial sperm whales (Cetacea, Odontoceti, Physeteroidea) from the Miocene of Peru. *Zool. J. Linn. Soc.* **179**, 404–474. (doi:10.1111/zoj.12456)
30. Kinkel MD, Thewissen JGM, Oelschläger HA. 2001 Rotation of middle ear ossicles during cetacean development. *J. Morphol.* **249**, 126–131. (doi:10.1002/jmor.1044)
31. Uhen MD. 2008 New protocetid whales from Alabama and Mississippi, and a new cetacean clade, Pelagiceti. *J. Vertebr. Paleontol.* **28**, 589–593. (doi:10.1671/0272-4634(2008)28[589:NPWFAA]2.0.CO;2)
32. de Muizon C. 1985 Nouvelles données sur le diphylétisme des Dauphins de rivière (Odontoceti, Cetacea, Mammalia). *Comptes rendus l'Academie des Sci. Série 2* **301**, 359–362.
33. Farina A, Lattanzi E, Malavasi R, Pieretti N, Piccioli L. 2011 Avian soundscapes and cognitive landscapes: theory, application and ecological perspectives. *Landsc. Ecol.* **26**, 1257–1267. (doi:10.1007/s10980-011-9617-z)
34. Nummela S, Reuter T, Hemilä S, Holmberg P, Paukku P. 1999 The anatomy of the killer whale middle ear (*Orcinus orca*). *Hear. Res.* **133**, 61–70. (doi:10.1016/S0378-5955(99)00053-2)
35. Hemilä S, Nummela S, Reuter T. 1999 A model of the odontocete middle ear. *Hear. Res.* **133**, 82–97. (doi:10.1016/S0378-5955(99)00055-6)
36. Hemilä S, Nummela S, Reuter T. 2010 Anatomy and physics of the exceptional sensitivity of dolphin hearing (Odontoceti: Cetacea). *J. Comp. Physiol* **196**, 165–179. (doi:10.1007/s00359-010-0504-x)
37. Mason MJ. 2016 Structure and function of the mammalian middle ear. II: Inferring function from structure. *J. Anat.* **228**, 300–312. (doi:10.1111/joa.12316)
38. Koyabu D, Hosojima M, Endo H. 2017 Into the dark: patterns of middle ear adaptations in subterranean eulipotyphlan mammals. *R. Soc. open sci.* **4**, 170608. (doi:10.1098/rsos.170608)
39. Árnason Ú, Gullberg A, Gretarsdottir S, Ursing B, Janke A. 2000 The mitochondrial genome of the sperm whale and a new molecular reference for estimating Eutherian divergence dates. *J. Mol. Evol.* **50**, 569–578. (doi:10.1007/s002390010060)
40. Árnason Ú, Lammers F, Kumar V, Nilsson MA, Janke A. 2018 Whole-genome sequencing of the blue whale and other rorquals finds signatures for introgressive gene flow. *Sci. Adv.* **4**, eaap9873. (doi:10.1126/sciadv.aap9873)
41. Zurano JP, Magalhães FM, Asato AE, Silva G, Bidau CJ, Mesquita DO, Costa GC. 2019 Cetartiodactyla: updating a time-calibrated molecular phylogeny. *Mol. Phylogenet. Evol.* **133**, 256–262. (doi:10.1016/j.ympev.2018.12.015)
42. Kellogg R. 1957 Two additional Miocene porpoises from the Calvert Cliffs, Maryland. *Proc. United States Natl Mus.* **108**, 279–337. (doi:10.5479/si.00963801.108-3387.279)
43. Kellogg R. 1968 Fossil marine mammals from the Miocene calvert formation of Maryland and Virginia, parts 5–8. *Bull. United States Natl. Mus.* **247**, 103–201.
44. Kellogg R. 1969 Cetothere skeletons from the Miocene choptank formation of Maryland and Virginia. *Bull. United States Natl. Mus.* **294**, 1–40. (doi:10.5479/si.03629236.294.1)
45. Westgate J, Whitmore FC. 2002 *Balaena ricei*, a new species of bowhead whale from the Yorktown formation (Pliocene) of Hampton, Virginia. In *Cenozoic mammals of land and Sea: tributes to the career of clayton E. Ray* (ed. RJ Emry), pp. 295–312. Smithsonian Contributions to Paleobiology. Washington, DC: Smithsonian Institution Press. (doi:10.5479/si.00810266.93)
46. Bianucci G. 2005 *Arimidelphis sorbinii* a new small killer whale-like dolphin from the Pliocene of Marecchia river (Central Eastern Italy) and a phylogenetic analysis of the Orcininae (Cetacea: Odontoceti). *Riv. Ital. di Paleontol. Stratigr.* **111**, 329–344. (doi:10.13130/2039-4942/6324)
47. Bianucci G, Vaiani SC, Casati S. 2009 A new delphinid record (Odontoceti, Cetacea) from the Early Pliocene of Tuscany (Central Italy): systematics and biostratigraphic considerations. *Neues Jahrb. Geol. Paläontol. Abh* **254**, 275–292. (doi:10.1127/0077-7749/2009/0018)
48. Bouetel V, de Muizon C. 2006 The anatomy and relationships of *Piscobalaena nana* (Cetacea, Mysticeti), a Cetotheriidae s.s. from the early Pliocene of Peru. *Geodiversitas* **28**, 319–395.
49. Bosselaers M, Post K. 2010 A new fossil rorqual (Mammalia, Cetacea, Balaenopteridae) from the

Early Pliocene of the North Sea, with a review of the rorqual species described by Owen and Van Beneden. *Geodiversitas* **32**, 331–363. (doi:10.5252/g2010n2a6)

50. Marx FG, Tsai C-H, Fordyce RE. 2015 A new Early Oligocene toothed 'baleen' whale (Mysticeti: Aetiocetidae) from western North America: one of the oldest and the smallest. *R. Soc. open sci.* **2**, 150476. (doi:10.1098/rsos.150476)
51. Boessenecker RW, Fordyce RE. 2017 A new eomysticetid from the Oligocene Kokoamu Greensand of New Zealand and a review of the Eomysticetidae (Mammalia, Cetacea). *J. Syst. Palaeontol.* **15**, 429–469. (doi:10.1080/14772019.2016.1191045)
52. Lambert O, Godfrey SJ, Fitzgerald EMG. 2019 *Yaquinacetus meadi*, a new latest Oligocene–early Miocene dolphin (Cetacea, Odontoceti, Squaloziphiidae, fam. nov.) from the Nye Mudstone (Oregon, USA). *J. Vertebr. Paleontol.* **38**, e1559174. (doi:10.1080/02724634.2018.1559174)
53. Fleischer G. 1973 Structural analysis of the Tympanicum complex in the bottlenosed dolphin (*Tursiops truncatus*). *J. Aud. Res.* **13**, 178–190.
54. Lillie DG. 1910 Observations on the anatomy and general biology of some members of the larger Cetacea. *Proc. Zool. Soc. Lond.* **80**, 769–792. (doi:10.1111/j.1096-3642.1910.tb01916.x)
55. Boisserie J-R, Fisher RE, Lihoreau F, Weston EM. 2011 Evolving between land and water: key questions on the emergence and history of the Hippopotamidae (Hippopotamoidea, Cetancodonta, Cetartiodactyla). *Biol. Rev.* **86**, 601–625. (doi:10.1111/j.1469-185X.2010.00162.x)
56. Wagner GP. 1995 The biological role of homologues: a building block hypothesis. *Neues Jahrb. Geol. Paläontol. Abh* **195**, 279–288. (doi:10.1127/njgpa/195/1995/279)
57. Wagner GP. 1996 Homologues, natural kinds and the evolution of modularity. *Am. Zool.* **36**, 36–43. (doi:10.1093/icb/36.1.36)
58. Eble GJ. 2005 Morphological modularity and macroevolution: conceptual and empirical aspects. In *Modularity: understanding the development and evolution of natural complex systems* (eds W Callebaut, D Rasskin-Gutman), pp. 221–238. Cambridge, MA: MIT Press. (doi:10.7551/mitpress/4734.001.0001)
59. Simpson GG. 1944 *Tempo and mode in evolution*. New York, NY: Columbia University Press.
60. Sienknecht UJ. 2013 Developmental origin and fate of middle ear structures. *Hear. Res.* **301**, 19–26. (doi:10.1016/j.heares.2013.01.019)
61. Burford CM, Mason MJ. 2016 Early development of the malleus and incus in humans. *J. Anat.* **229**, 857–870. (doi:10.1111/joa.12520)
62. Reichert C. 1837 Ueber die Visceralbogen der Wirbelthiere im Allgemeinen und deren Metamorphosen bei den Vögeln und Säugethieren. *Arch. Anat. Physiol. Wissenschaftliche Med.* (*Leipzig*) **1837**, 120–222.
63. Luo Z-X. 2007 Transformation and diversification in early mammal evolution. *Nature* **450**, 1011–1019. (doi:10.1038/nature06277)
64. Luo Z-X. 2011 Developmental patterns in Mesozoic evolution of mammal ears. *Annu. Rev. Ecol. Evol. Syst.* **42**, 355–380. (doi:10.1146/annurev-ecolsys-032511-142302)
65. Maier W, Ruf I. 2016 Evolution of the mammalian middle ear: a historical review. *J. Anat.* **228**, 270–283. (doi:10.1111/joa.12379)
66. Anthwal N, Thompson H. 2016 The development of the mammalian outer and middle ear. *J. Anat.* **228**, 217–232. (doi:10.1111/joa.12344)
67. Thompson H, Ohazama A, Sharpe PT, Tucker AS. 2012 The origin of the stapes and relationship to the otic capsule and oval window. *Dev. Dyn.* **241**, 1396–1404. (doi:10.1002/dvdy.23831)
68. Nummela S, Thewissen JGM. 2008 The physics of sound in air and water. In *Sensory evolution on the threshold: adaptations in secondarily aquatic vertebrates* (eds JGMH Thewissen, S Nummela), pp. 174–181. Berkeley, CA: University of California Press.
69. Nummela S. 2008 Hearing in aquatic mammals. In *Sensory evolution on the threshold: adaptations in secondarily aquatic vertebrates* (eds JGMH Thewissen, S Nummela), pp. 210–224. Berkeley, CA: University of California Press. (doi:10.1525/california/9780520252783.003.0013)
70. Burda H, Bruns V, Hickman GC. 1992 The ear in subterranean insectivora and rodentia in comparison with ground-dwelling representatives. I. Sound conducting system of the middle ear. *J. Morphol.* **214**, 49–61. (doi:10.1002/jmor.1052140104)
71. Hetherington T. 2008 Comparative anatomy and function of hearing in aquatic amphibians, reptiles, and birds. In *Sensory evolution on the threshold: adaptations in secondarily aquatic vertebrates* (eds JGMH Thewissen, S Nummela), pp. 182–209. Berkeley, CA: University of California Press. (doi:10.1525/california/9780520252783.003.0012)
72. Kastak D, Schusterman RJ. 1998 Low-frequency amphibious hearing in pinnipeds: methods, measurements, noise, and ecology. *J. Acoust. Soc. Am.* **103**, 2216–2228. (doi:10.1121/1.421367)
73. Kastak D, Schusterman RJ. 1999 In-air and underwater hearing sensitivity of a northern elephant seal (*Mirounga angustirostris*). *Can. J. Zool.* **77**, 1751–1758. (doi:10.1139/z99-151)
74. Wartzok D, Ketten DR. 1999 Marine mammal sensory systems. In *Biology of marine mammals* (eds JE Reynolds II, SA Rommel), pp. 117–136. Washington, DC: Smithsonian Institution Press.
75. Hemilä S, Nummela S, Berta A, Reuter T. 2006 High-frequency hearing in phocid and otariid pinnipeds: an interpretation based on inertial and cochlear constraints. *J. Acoust. Soc. Am.* **120**, 3463–3466. (doi:10.1121/1.2372712)
76. Sills JM, Southall BL, Reichmuth C. 2014 Amphibious hearing in spotted seals (*Phoca largha*): underwater audiograms, aerial audiograms and critical ratio measurements. *J. Exp. Biol.* **217**, 726–734. (doi:10.1242/jeb.097469)
77. Sills JM, Southall BL, Reichmuth C. 2015 Amphibious hearing in ringed seals (*Pusa hispida*): underwater audiograms, aerial audiograms and critical ratio measurements. *J. Exp. Biol.* **218**, 2250–2259. (doi:10.1242/jeb.120972)
78. Loza CM, Krmpotic CM, Galliari FC, Andrés Laube PF, Negrete J, Scarano AC, Loureiro J, Carlini AA, Barbeito CG. 2019 Adaptations to a semiaquatic lifestyle in the external ear of southern pinnipeds (Otariidae and Phocidae, Carnivora): morphological evidences. *Zoology* **133**, 66–80. (doi:10.1016/j.zool.2019.02.006)
79. Mourlam MJ, Orliac MJ. 2019 Data from: Early evolution of the ossicular chain in Cetacea: into the middle ear gears of a semi-aquatic protocetid whale. Dryad Digital Repository. (doi:10.5061/dryad.0k3fv2j)